RESEARCH ARTICLE

Stepwise Functional Brain Architecture Correlates with Atrophy in Progressive Supranuclear Palsy

Edoardo Gioele Spinelli, MD, PhD,[1,2,3] Alma Ghirelli, MD,[1,2,3] Ilaria Bottale, MD,[1,2,3] Silvia Basaia, PhD,[1] Elisa Canu, PhD,[1] Veronica Castelnovo, PhD,[1] Maria Antonietta Volontè, MD,[3] Sebastiano Galantucci, MD, PhD,[3] Giuseppe Magnani, MD,[3] Francesca Caso, MD, PhD,[3] Giordano Cecchetti, MD, PhD,[1,3,4] Paola Caroppo, MD, PhD,[5] Sara Prioni, MSc,[5] Cristina Villa, PhD,[5] Keith A. Josephs, MD, MST, MSc,[6] Jennifer L. Whitwell, PhD,[7] Massimo Filippi, MD,[1,2,3,4,8] and Federica Agosta, MD, PhD[1,2,3*]

[1]*Neuroimaging Research Unit, Division of Neuroscience, IRCCS San Raffaele Scientific Institute, Milan, Italy*
[2]*Vita-Salute San Raffaele University, Milan, Italy*
[3]*Neurology Unit, IRCCS San Raffaele Scientific Institute, Milan, Italy*
[4]*Neurophysiology Service, IRCCS San Raffaele Scientific Institute, Milan, Italy*
[5]*Unit of Neurology 5—Neuropathology, Fondazione IRCCS Istituto Neurologico Carlo Besta, Milan, Italy*
[6]*Department of Neurology, Mayo Clinic, Rochester, Minnesota, USA*
[7]*Department of Radiology, Mayo Clinic, Rochester, Minnesota, USA*
[8]*Neurorehabilitation Unit, IRCCS San Raffaele Scientific Institute, Milan, Italy*

ABSTRACT: Background: Stepwise functional connectivity (SFC) detects whole-brain functional couplings of a selected region of interest at increasing link-step topological distances.

Objective: This study applied SFC to test the hypothesis that stepwise architecture propagating from the disease epicenter would shape patterns of brain atrophy in patients with progressive supranuclear palsy–Richardson's syndrome (PSP-RS).

Methods: Thirty-six patients with PSP-RS and 44 age-matched healthy control subjects underwent brain magnetic resonance imaging on a 3-T scanner. The disease epicenter was defined as the peak of atrophy observed in an independent cohort of 13 cases with postmortem confirmation of PSP pathology and used as seed region for SFC analysis. First, we explored SFC rearrangements in patients with PSP-RS, as compared with age-matched control subjects. Subsequently, we tested SFC architecture propagating from the disease epicenter as a determinant of brain atrophy distribution.

Results: The disease epicenter was identified in the left midbrain tegmental region. Compared with age-matched control subjects, patients with PSP-RS showed progressively widespread decreased SFC of the midbrain with striatal and cerebellar regions through direct connections and sensorimotor cortical regions through indirect connections. A correlation was found between average link-step distance from the left midbrain in healthy subjects and brain volumes in patients with PSP-RS ($r = 0.38$, $P < 0.001$).

Conclusions: This study provides comprehensive insights into the topology of functional network rearrangements in PSP-RS and demonstrates that the brain architectural topology, as described by SFC propagating from the disease epicenter, shapes the pattern of atrophic changes in PSP-RS. Our findings support the

*__Correspondence to:__ Dr. Federica Agosta, Neurology Unit and Neuroimaging Research Unit, Division of Neuroscience, IRCCS San Raffaele Scientific Institute, Vita-Salute San Raffaele University, Via Olgettina 60, 20132 Milan, Italy; E-mail: agosta.federica@hsr.it

Relevant conflicts of interest/financial disclosures: E.G.S. was cofinanced by the Next Generation EU (DM 1557 11.10.2022). J.L.W. was supported by the National Institutes of Health (R01-NS89757) and the Dana Foundation. F.A. was supported by the European Research Council (StG-2016_714388_NeuroTRACK) and Foundation Research on Alzheimer Disease.

The views and opinions expressed are only those of the authors and do not necessarily reflect those of the European Union or the European Commission. Neither the European Union nor the European Commission can be held responsible for them.

Funding agencies: This study was supported by the European Research Council (StG-2016_714388_NeuroTRACK); Foundation Research on Alzheimer Disease; Next Generation EU, in the context of the National Recovery and Resilience Plan, Investment PE8—Project Age-It: "Ageing Well in an Ageing Society"; National Institutes of Health (R01-NS89757); and Dana Foundation.

Full financial disclosures and author roles may be found in the online version of this article.

Received: 19 February 2024; **Revised:** 19 May 2024; **Accepted:** 28 May 2024

Published online 17 June 2024 in Wiley Online Library (wileyonlinelibrary.com). DOI: 10.1002/mds.29887

view of a network-based pathology propagation in this primary tauopathy. © 2024 The Author(s). *Movement Disorders* published by Wiley Periodicals LLC on behalf of International Parkinson and Movement Disorder Society.

Key Words: progressive supranuclear palsy; MRI; resting-state functional MRI; RS fMRI; stepwise functional connectivity; SFC

Progressive supranuclear palsy (PSP) is a relentless neurodegenerative condition characterized by a progressive decline in motor function, oculomotor paralysis, speech alterations, and cognitive deficits.[1] Due to overlapping symptoms with other Parkinsonian syndromes, PSP presents unique challenges for its clinical management and comprehension of underlying pathophysiology. Despite some variability in the pathological substrate of PSP syndrome, cases presenting with a typical Richardson's syndrome (PSP-RS) are associated with the deposition of characteristic four-repeat tau aggregates in the brain, posing this condition of the frontotemporal lobar degeneration (FTLD) spectrum as an in vivo model of tauopathy.[2]

There is a consistent overlap between atrophy patterns observed in patients with neurodegenerative conditions and intrinsic connectivity networks in healthy individuals.[3,4] Therefore, neurodegenerative processes are thought to originate in specific focal points (ie, disease epicenters) and subsequently propagate through highly interconnected neural networks. Magnetic resonance imaging (MRI) connectomics has unveiled the relationship between brain connectivity networks and the progressive accumulation of pathology in various disorders within the FTLD spectrum, including PSP.[5-7] These findings lend support to the prevailing perspective of a network-based model for the spread of pathogenic protein deposits.

Prior studies have mainly used traditional functional brain connectivity analyses that do not distinguish between direct and indirect connections to the disease epicenter. Stepwise functional connectivity (SFC) overcomes traditional connectomic approaches, reconstructing a hierarchical architecture of the functional connectome from a region of interest (ROI) that includes and differentiates direct and indirect connections.[8] This technique has provided an interesting framework to assess the spatial convergence between the functional topological organization and the pathological burden in neurodegenerative diseases, supporting a network-based degeneration hypothesis for Alzheimer's disease, Parkinson's disease, and frontotemporal dementia.[5,9,10]

The purpose of this study was to investigate disease-specific rearrangements of SFC in patients with PSP-RS, and to test brain network architecture propagating from the disease epicenter as a determinant of atrophy distribution.

Subjects and Methods

Participants

Main Cohort

Between March 2010 and April 2022, 64 patients with a suspected PSP syndrome were referred to the Neurology Unit, IRCCS San Raffaele Scientific Institute in Milan to undergo neurological examination, neuropsychological assessment, and brain MRI scan on a 3-T scanner. Forty-six patients were diagnosed with probable PSP-RS, according to current diagnostic criteria.[11] Ten patients were excluded because of the presence of a high cerebrovascular burden, severe motion artifacts, or incomplete MRI protocols, resulting in 36 patients with PSP-RS to be included in this study.

Forty-four healthy control subjects (HCs), comparable for age and sex with patients (therefore named HC-old), were recruited among spouses of patients and by word of mouth. Control subjects showed normal neurological assessment, Mini-Mental State Examination (MMSE)[12] score ≥ 27, and no family history of neurodegenerative diseases. In addition to patients with PSP-RS and HC-old subjects, 50 young healthy control subjects (HC-young, ie, aged 20–30 years, 23 females) were recruited to provide as a reference healthy connectome for association analysis between SFC maps and regional atrophy in patients with PSP-RS, excluding the influence of age-related connectome alterations.

Path-Proven Cohort

MRI data of 13 patients with PSP-RS and postmortem histological evidence of 4R-tau PSP pathology were provided by the Neurodegenerative Research Group, Mayo Clinic in Rochester (MN, USA) to identify the disease epicenter to be used as seed of the SFC analysis performed on the main study cohort. T1-weighted scans obtained in vivo between April 2007 and September 2018 were used. Disease duration at MRI of the path-proven cohort (3.73 ± 1.57 years) and the main study cohort (3.24 ± 1.54 years) were comparable ($P = 0.31$). Thirteen age- and sex-matched HCs were also selected. The inclusion and exclusion criteria for HCs were the same as for the main cohort.

Table 1 summarizes the demographic characteristics of the study cohorts. The study methods were authorized by local ethical standards committees on human testing, and all subjects supplied signed informed permission.

TABLE 1 *Demographic and clinical features of the subjects included in this study*

Main cohort	**HC-Old**	**PSP-RS**	***P***
n	44	36	
Age at MRI, y	70.19 ± 4.56 (60.79–79.34)	71.57 ± 7.74 (52–85.25)	0.33
Sex, M/F	17/27	13/23	1.00
Education, y	12.25 ± 4.39 (5–24)	9.44 ± 4.11 (5–23)	**0.005**
Disease duration, y	–	3.24 ± 1.54 (0.82–8.23)	–
Scanner type, 1/2	17/27	16/20	0.65
UPDRS III motor score—*off*	–	38.27 ± 13.48 (23–75)	–
H&Y	–	3.1 ± 0.69 (2–4)	–
MMSE	29.16 ± 0.9 (27–30)	25.50 ± 3.06 (18–30)	**<0.001**
Path-proven cohort	**HC**	**PSP-RS**	***P***
n	13	13	
Age at MRI, y	62.62 ± 7.11 (55–77)	66.19 ± 7.24 (53.5–76.7)	0.22
Sex, M/F	4/9	8/5	0.24
Education, y	14.31 ± 1.97 (12–18)	14.83 ± 1.99 (12–18)	0.51
Disease duration, y	–	3.73 ± 1.57 (1.64–6.89)	–
UPDRS III motor score	–	45.4 ± 10.5	–
MMSE	–	27.58 ± 1.98 (24–30)	–

Values are means ± SD (range). *P* values refer to ANOVA models, Bonferroni-corrected for multiple comparisons, or Fisher's exact test, as appropriate. The threshold of statistical significance was set at $P < 0.05$.
Abbreviations: HC, healthy control subject; PSP-RS, progressive supranuclear palsy–Richardson's syndrome; MRI, magnetic resonance imaging; M, male; F, female; UPDRS, Unified Parkinson's Disease Rating Scale Part III; H&Y, Hoehn and Yahr; MMSE, Mini-Mental State Examination; PSP, progressive supranuclear palsy.

Clinical Evaluation

Clinical evaluation of the main cohort was performed at the IRCCS San Raffaele Scientific Institute by experienced neurologists blinded to the MRI results. Patients with PSP-RS were evaluated through the Unified Parkinson's Disease Rating Scale Part III ((UPDRS III), with all the dopaminergic medications withheld overnight prior to testing (UPDRS III motor score *off*),[13] and Hoehn and Yahr Scale.[14]

Neuropsychological Assessment

Participants underwent a comprehensive neuropsychological assessment performed by experienced neuropsychologists. Global cognitive functioning was evaluated with the MMSE,[12] whereas memory, attentive-executive, visuospatial, linguistic, emotional, and behavioral domains were evaluated using specific tests (see Supporting Information).

MRI Acquisition

Patients and control subjects from the main cohort underwent a brain scan including three-dimensional T1-weighted and resting-state functional MRI (RS fMRI) sequences on a 3-T scanner (Philips Medical Systems, Best, the Netherlands) at the IRCCS San Raffaele Scientific Institute between 2007 and 2019. The original scanner was substituted with an upgraded model from the same manufacturer in 2016. Patients of the Mayo Clinic cohort also underwent a 3-T brain MRI, including a three-dimensional T1-weighted sequence on one of two GE scanners (GE Healthcare, Milwaukee, WI, USA). MRI protocols are summarized in Table S1.

MRI Analysis

The MRI analysis was performed at the Neuroimaging Research Unit, IRCCS San Raffaele Scientific Institute by experienced observers, blinded to subjects' identity.

Voxel-Based Morphometry

Voxel-based morphometry (VBM) analysis was performed using SPM12 (http://www.fil.ion.ucl.ac.uk/spm/) and Diffeomorphic Anatomical Registration Exponentiated

Lie Algebra (DARTEL) registration method,[15] to assess brain volumetric alterations[5] and identify the disease epicenter in path-proven PSP from the Mayo Clinic cohort. Considering that subcortical regions mostly affected in patients with PSP pathology are best sampled by the white matter (WM) parcellation of VBM,[16] we performed both gray matter (GM) and WM parcellations. Group comparisons between patients and HCs of the path-proven cohort were tested using analysis of variance (ANOVA) models. Using the MarsBaR ROI toolbox for SPM12 (http://marsbar.sourceforge.net), a spherical, 10-mm-radius ROI was created around the most significant atrophy peak. The choice of using an independent set of patients with PSP with proven pathology for seed definition was made to avoid circular reasoning when correlating atrophy with SFC data.

SFC Analysis

In brief, SFC is a graph-theory-based method that allows to map the connectivity patterns of selected brain seed regions at different step (or link-step) distances, creating a framework where a step refers to the number of links (edges) that belong to a path connecting a node to the seed.[8] Here, we will use the term *direct* connections when assessing one-step functional topological distances (step 1), whereas the term *indirect* will refer to further-step distances from the seed region (steps 2–4). The pipeline adopted for this study has been recently described.[5,10] Notably, the number of steps merely describes the topological distance between two nodes within the brain functional connectome; therefore, it does not refer to the presence of a direct/indirect axonal connection.

In patients with PSP-RS and each group of HCs (ie, HC-old and HC-young) of the main cohort, SFC analysis was performed using as seed region the specific ROI previously identified in the Mayo Clinic population. Given the lack of directionality information provided by RS fMRI data, we did not include any restrictions about recurrent pathways crossing the seed regions multiple times. All maps across different link-step distances from 1 to 4 were used to describe connectivity differences between HC-old and PSP-RS participants. Further steps were not included in this analysis, as SFC patterns became stable for link-step distances above 4. Subsequently, a combined version of all SFC 1 to 4 maps into one single map from nondisrupted connectivity pathways of HC-young (combined SFC map) was employed to investigate the relationships between "standard" healthy neuroimaging patterns and volumetric measures of patients with PSP. To build the SFC combined map, we determined, for each pair of voxels, at which step the relative degree of stepwise connectivity was maximized. Thus, we obtained an SFC combined map for each subject, with values ranging from 1 to 4. Finally, the combined SFC map was registered to the 90-region Automated Anatomical Labeling (AAL) atlas.

Regional Brain Volumetric Measures

To obtain measures of regional atrophy in patients with PSP-RS from the main cohort, we parcellated GM maps of these subjects into the 90 AAL ROIs. Cortical GM maps were obtained using the segmentation step of VBM, whereas maps of the basal ganglia, hippocampus, and amygdala were obtained using the FMRIB's Integrated Registration and Segmentation Tool (FIRST) (http://www.fmrib.ox.ac.uk/fsl/first/index.html). The AAL atlas was then registered to the subject T1-weighted images, masked using the GM maps, by means of linear (FLIRT)[17] and nonlinear (FNIRT)[18] registrations in FSL. Regional brain volumes were obtained and multiplied by the normalization factor derived from SIENAx (http://www.fmrib.ox.ac.uk/fsl/sienax/index.html) to correct for individual head size. The volumetric values of each AAL region for each patient were normalized relative to controls.

Statistical Analysis

Sociodemographic, Clinical, and Cognitive Data

The normal distribution assumption was tested using the Q-Q plot, as well as the Shapiro–Wilks and Kolmogorov–Smirnov tests. Fisher's exact test or ANOVA models were used to evaluate demographic, clinical, and neuropsychological data between groups, as appropriate. ANOVA models were adjusted for age, sex, and education, Bonferroni-corrected for multiple comparisons. The statistical significance level was chosen at $P < 0.05$. The program SPSS Statistics 26.0 was used.

MRI Data

VBM group comparisons were assessed using an ANOVA model adjusted for total intracranial volume, age, and sex, thresholded at $P < 0.05$, family-wise error (FWE)-corrected for multiple comparisons, as implemented in SPM12. Voxel-wise studies were undertaken to examine SFC alterations using general linear models implemented in SPM12. Whole-brain two-sample t test comparisons were done for each of the four stages, with age, sex, and scanner type as covariates. To detect statistically significant differences at $P < 0.05$, FWE-corrected, we used a threshold-free cluster enhancement method combined with nonparametric permutation testing (5000 permutations), as implemented in the Computational Anatomy Toolbox 12 (CAT12, http://www.neuro.uni-jena.de/cat/). Finally, for each AAL region, correlations between the combined SFC maps obtained in HC-young subjects for the

seed ROI and average brain volumes of patients with PSP-RS of the main sample were tested using the Pearson correlation coefficient (SPSS Statistics 26.0).

Results

Sociodemographic, Clinical, and Neuropsychological Features

Patients with PSP-RS and respective HCs of each cohort were comparable in terms of age at MRI, sex, and scanner type (Table 1).

Patients with PSP-RS of the main cohort had lower education levels than age-matched HCs. They had mean disease duration of approximately 3 years and were in a moderate stage of the disease (mean Hoehn and Yahr Scale score = 3.1 ± 0.7). They showed a mild to moderate cognitive impairment, as measured by MMSE scores (mean = 25.5 ± 3.1). After adjusting for age, sex, and education levels, patients with PSP-RS showed significant impairment across all assessed cognitive domains (Table S2), including verbal and visual memory, attention, executive functions, visuospatial abilities, phonemic and semantic fluency, as well as emotional cognition. Mood was also mildly affected (Table S2).

Identification of Disease Epicenter

VBM analysis of path-proven PSP patients of the Mayo Clinic cohort showed one cluster of significant atrophy involving the midbrain tegmental and subthalamic regions, bilaterally ($P < 0.05$, FWE-corrected; Fig. 1A), with the peak of significance located in the left midbrain (T score = 8.8; Montreal Neurological Institute coordinates = −8, −12, −3). This region was selected as seed region for the subsequent SFC analysis (Fig. 1B).

SFC Comparisons

We tested SFC differences between patients with PSP-RS and HC-old of the main cohort ($P < 0.05$, FWE-corrected, Fig. 2).

Direct Connectivity (Step 1)

At one link-step distance, the seed ROI placed in the left midbrain of patients with PSP-RS showed reduced SFC (yellow-red regions in Fig. 2) with left precentral, postcentral, superior frontal, inferior frontal, lingual and supramarginal gyri, the left insula and head of the caudate nucleus, as well as the anterior cingulate and pericalcarine cortices, bilaterally—with a greater involvement of the left hemisphere. Decreased SFC of the left midbrain was also found with bilateral anterior cerebellar regions, including lobules IV, V, and VI (mostly in the right hemispheric regions), and the vermis. Patients with PSP-RS showed increased direct SFC of the left midbrain (blue-green in Fig. 2) with its surrounding regions in the midbrain, the subthalamic/hypothalamic regions, rostral anterior cingulate, medial orbitofrontal gyrus, cuneus, and lateral occipital and anterior temporal cortices, bilaterally.

Indirect Connectivity (Steps 2–4)

Across steps 2–4, patients with PSP-RS relative to HC-old showed decreased SFC of the left midbrain with extensive cortical regions, including the bilateral

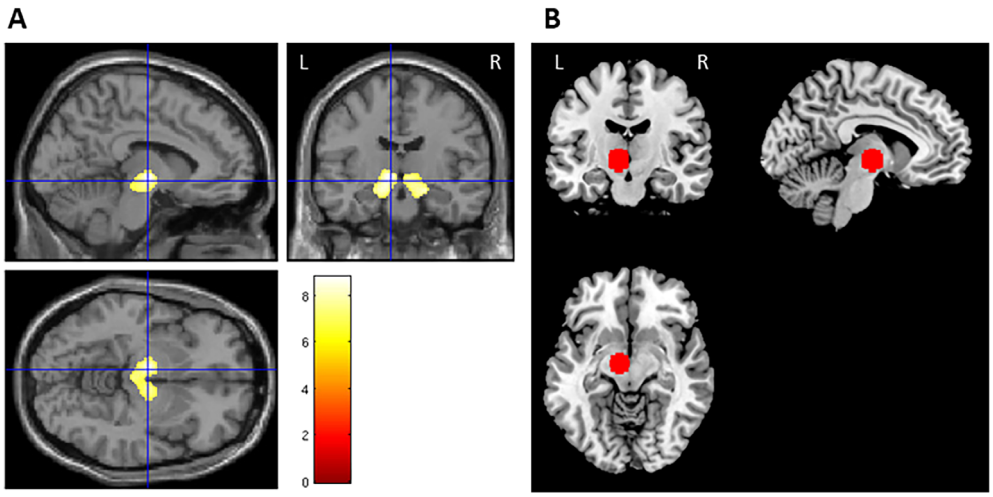

FIG. 1. Identification of disease epicenter. (**A**) Results of voxel-based morphometry analysis showing regions of significant brain atrophy in path-proven PSP-RS patients of the Mayo Clinic cohort when compared with healthy control subjects. Significant clusters are overlaid on the axial sections of the Montreal Neurological Institute (MNI) standard brain. Analyses were corrected for age, sex, and total intracranial volume. Statistical threshold for significance was $P < 0.05$, FWE-corrected for multiple comparisons. (**B**) A 10-mm-radius sphere overlaid on the MNI standard brain shows the identified peak of atrophy in the left midbrain. FWE, family-wise error; L, left hemisphere; PSP-RS, progressive supranuclear palsy–Richardson's syndrome; R, right hemisphere. [Color figure can be viewed at wileyonlinelibrary.com]

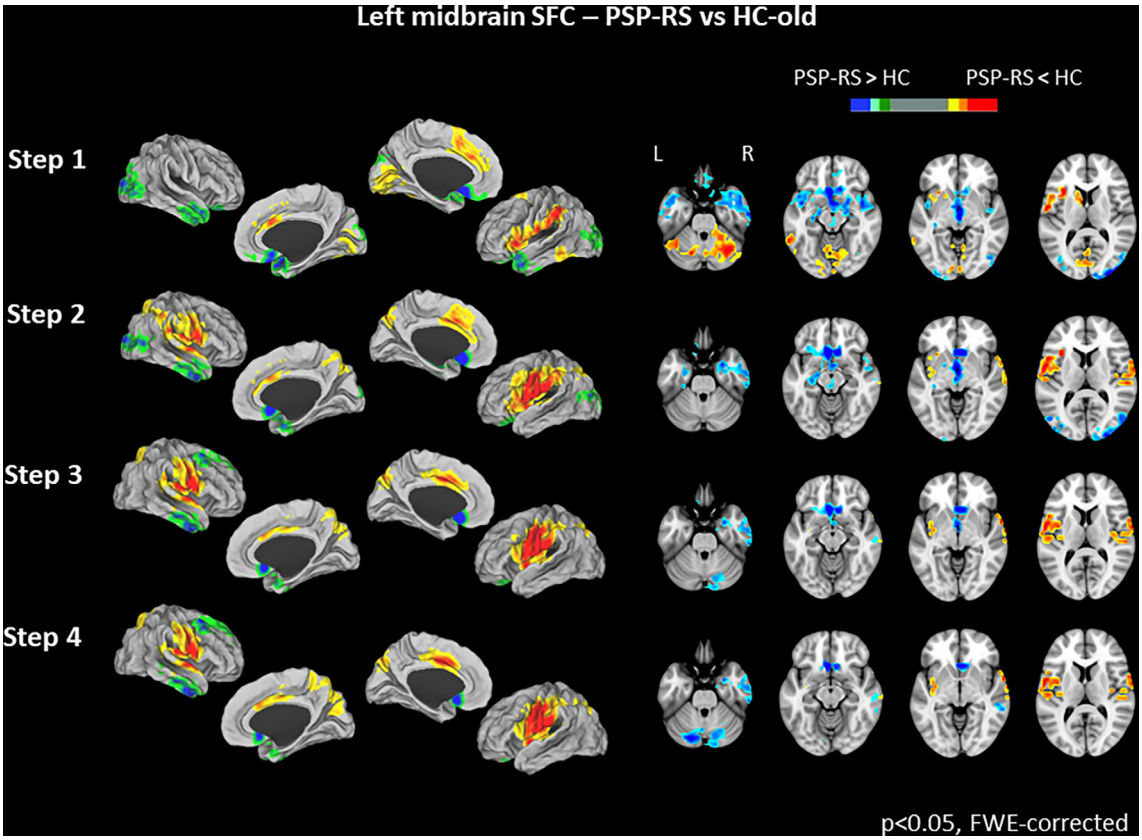

FIG. 2. Stepwise functional connectivity (SFC) alterations in patients with PSP-RS. Cortical and subcortical differences between patients with PSP-RS and age-matched healthy control subjects (HC-old) from the main cohort in SFC of the left midbrain (red-yellow = lower functional connectivity, blue-green = higher functional connectivity). Statistical threshold for significance was $P < 0.05$, FWE-corrected for multiple comparisons. FWE, family-wise error; HC, healthy control subject; L, left hemisphere; PSP-RS, progressive supranuclear palsy–Richardson's syndrome; R, right hemisphere. [Color figure can be viewed at wileyonlinelibrary.com]

anterior cingulate, precentral, postcentral, insular, supramarginal, inferior parietal, and precuneal cortices, as well as the left superior frontal cortex. In step 2, patients with PSP-RS showed increased SFC of the left midbrain with the same regions as in step 1, with a lesser involvement of the left anterior temporal regions. In steps 3 and 4, increased SFC of the midbrain involved the medial orbitofrontal cortex, bilaterally, the right superior frontal cortex, and the right anteroinferior temporal regions. In steps 3 and 4, patients with PSP-RS also showed increased SFC of the left midbrain with bilateral regions of the posterior cerebellum (crus I, crus II, and lobule VIIb).

Correlations Between Brain Atrophy and SFC Architecture

The left midbrain ROI was also used to create an SFC model of brain network architecture in the HC-young group, as represented in Fig. 3. Combining the average SFC maps of steps 1–4, we determined, for each region of the AAL atlas, at which functional link-step distance from the left midbrain they were more likely to stand. Table S3 and Figure S1 provide the full list of AAL regions—grouped by brain anatomical areas—at progressive link-step distances from the PSP disease epicenter. For each brain region, we found a significant correlation between average SFC link-step distance from the left midbrain in HC-young and normalized mean volumes in patients with PSP-RS of the main cohort (Fig. 4, $r = 0.40$, $P < 0.001$).

Discussion

SFC has been recently developed to investigate the organization of functional connectivity (FC) pathways at discrete numbers of relay stations in several neurological and psychiatric conditions.[9] In this study, we tested such hierarchical models of brain functional network architecture to assess rearrangements propagating from a disease epicenter identified in the midbrain in a cohort of patients with PSP-RS. Our results showed a widespread decreased SFC of the epicenter with ipsilateral sensorimotor, striatal, and anterior cerebellar regions through direct connections, progressively involving also bilateral sensorimotor cortical regions through indirect connections. This finding was mirrored by a more

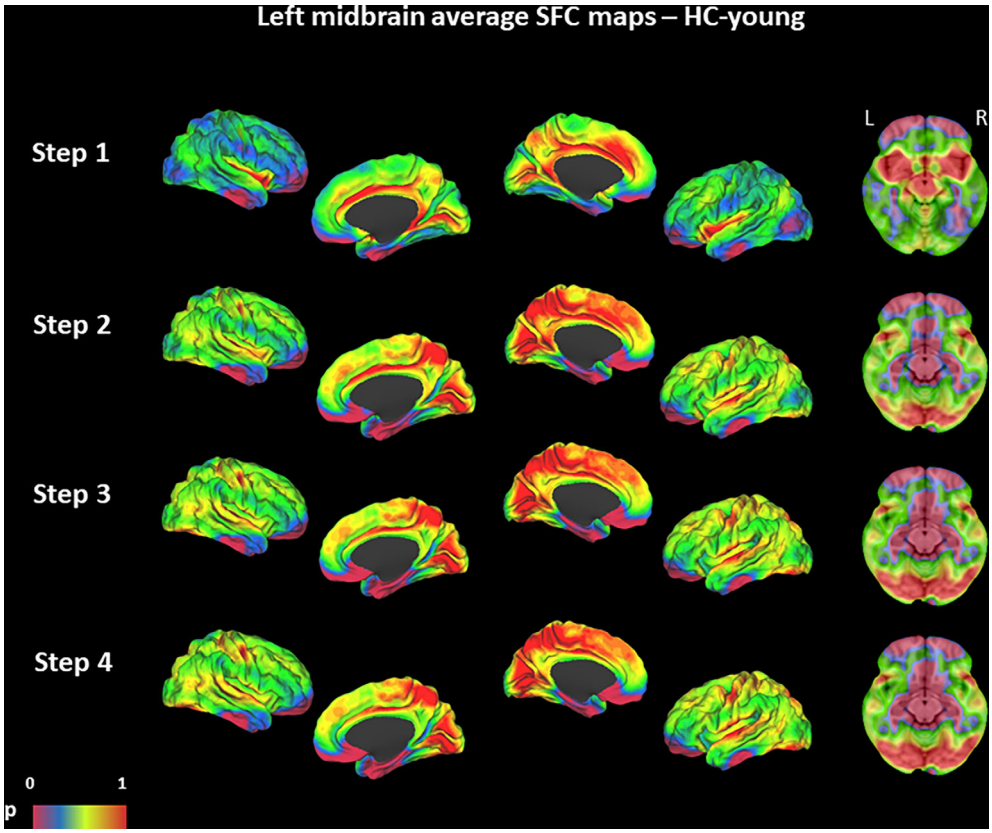

FIG. 3. Stepwise functional connectivity (SFC) architecture from disease epicenters in young healthy subjects. Average SFC maps in young healthy control subjects (HC-young) using the left midbrain as seed region of interest. Results are depicted in surface space. Red-yellow indicates high strength of connectivity; blue-violet indicates low strength of connectivity. [Color figure can be viewed at wileyonlinelibrary.com]

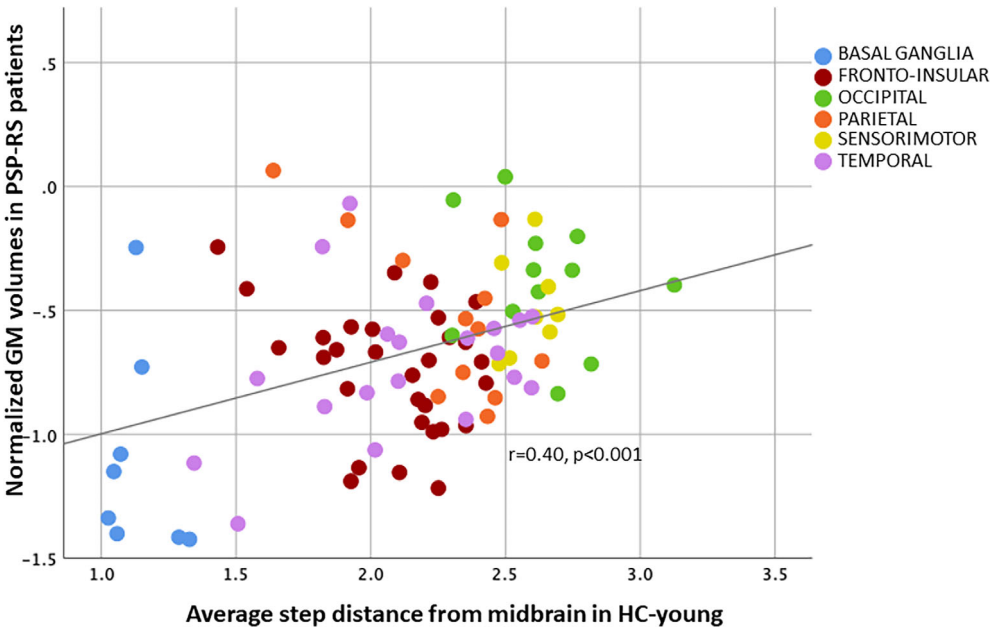

FIG. 4. Correlation analysis between average step distance from the left midbrain in HC-young subjects and average volume in patients with PSP-RS from the main cohort for each of the 90 brain regions of the AAL atlas. Color legend represents regional distribution of each AAL label. AAL, Automated Anatomical Labeling; GM, gray matter; HC, healthy control subject; PSP-RS, progressive supranuclear palsy–Richardson's syndrome. [Color figure can be viewed at wileyonlinelibrary.com]

circumscribed pattern of increased SFC of the midbrain with extramotor cortical, subcortical, and posterior cerebellar regions. The correlation analysis suggested that the brain architectural topology, as described by SFC link-steps propagating from the disease epicenter, shaped the pattern of atrophic changes in patients with PSP-RS, supporting the view of a network-based pathology propagation in this primary tauopathy.

We identified as disease epicenter the rostral area of the midbrain tegmentum, close to the subthalamic nucleus, as derived from the peak of atrophy of an independent cohort of patients with PSP-RS with postmortem histopathological diagnosis of PSP pathology. The location of our seed ROI was consistent with the known midbrain atrophy[16,19-22] and deposition of tau pathology in this region.[23-25] The location of our seed ROI was also in line with the recently proposed pathological staging system,[24] which considers the midbrain/subthalamic regions among those involved in the earliest stages of the disease. A previous study assessing structural MRI connectomics to model pathology spreading in PSP[7] indicated a seed located in the hypothalamus as the best candidate for explaining disease pathological spread of tau pathology. Compared with this previous study,[7] our results benefited not only from an unbiased identification of the disease epicenter from an independent pathologically proven cohort, but also from a more accurate clinical classification that led to the inclusion of only patients with PSP-RS, because other phenotypes (eg, PSP with prevalent parkinsonism) show important divergence in the distribution of 4R-tau pathology.[26]

To the best of our knowledge, this was the first research to employ SFC analysis in the context of PSP. The novelty of our approach, which has been recently applied to other phenotypes of the FTLD spectrum,[5] lies in the possibility to apply the same technique for the double-fold purpose to evaluate any divergence in functional rearrangements affecting direct and indirect connections with the disease epicenter, as well as to model the brain network architecture as a determinant of the progression of disease pathology.

When we evaluated SFC reorganization in patients with PSP-RS, as compared with age-matched controls, a significant decrease in direct SFC was found between the left midbrain epicenter and widespread brain regions broadly involved in motor planning and processing. The involvement of ipsilateral cortical and subcortical brain areas, such as the primary motor, supplementary motor, and premotor cortices, as well as the ipsilateral caudate nucleus and (mostly, contralateral) anterior cerebellar regions, is consistent with an early disruption of nigrostriatal, motor cerebellar, and cortical sensorimotor circuits shown by different neuroimaging studies in patients with PSP.[27-33] Previous fMRI studies have observed similar abnormalities,[27-29,34] with a widespread reorganization of functional connectivity in motor networks involving the precentral and premotor cortices, supplementary motor area, striatum, and anterior cerebellar regions, where structural changes were also observed.[35] Overall, these findings support the hypothesis of a functional disconnection caused by structural damage along the dentatorubrothalamic and nigrostriatal tracts,[36] crucially involved in the pathogenesis of PSP motor symptoms.

The significant decrease in SFC between the midbrain and anterior cingulate/insular cortical regions through both direct and indirect connections is consistent with a disruption of the salience network, likely propagating from its subcortical nodes, as previously suggested.[36] The decreased direct SFC with the pericalcarine cortex is in agreement with an early involvement of posterior thalamic radiations described by structural MRI studies.[37,38]

The pattern of decreased functional connectivity observed in patients with PSP-RS became even more widespread at increasing link-step distances from the midbrain, with greater disconnection with bihemispheric frontal, parietal, and anterior cingulate regions, supporting the hypothesis that the failure of functional integrity observed in the FTLD spectrum may result from widespread downstream propagation effects of disconnection from the disease epicenter at increasing topological distances.[39,40]

One of the most striking results in our study was the increased SFC of the midbrain epicenter with immediately surrounding regions, similar to previous findings in other FTLD variants.[5] Based on the fact that increased local functional connectivity could be observed since link-step 1, our hypothesis is that structural alterations may drive network disruptions, probably because of a loss of local inhibitory control.[41] Following this line of thought, this phenomenon might therefore reflect a maladaptive process caused by local deafferentation, as a response to pathological tau spreading.[42] The presence of increased SFC with limbic cortical areas (ie, medial orbitofrontal, anterior temporal, cingulate) and association with emotional lability in patients with PSP[43] is further supportive of this notion. By contrast, the increased SFC of the midbrain epicenter with the contralateral superior frontal cortical regions of the frontal eye field at higher link-step distances might rather suggest a possible compensatory role for impaired control of eye movements,[42,44] the pathognomonic clinical feature of PSP.[11] Increased SFC of the midbrain with the medial prefrontal cortex, which was present throughout all link-steps, has also been previously described and suggested as a possible compensatory element.[45] In line with this view, a previous connectomic study performed in a smaller cohort of patients with PSP-RS[6] suggested that impaired cortico-subcortical functional connectivity might result in cerebral information transfer taking a less direct path through a larger number of cortical nodes, causing

widespread increases in cortical functional connectivity to compensate for tau aggregation burden in subcortical regions.

Notably, in contrast with the extensively decreased direct SFC of the midbrain with anterior cerebellar regions (ie, lobules IV–VI and vermis)—mostly involved in motor planning and modulation and typically atrophied in PSP[46]—at indirect link-steps, we observed a significant increased SFC with posterior cerebellar regions (ie, crus I, crus II, and lobule VIIb), which recent neuroimaging studies have linked with the elaboration of action sequences relevant to social cognition and theory of mind.[47,48] This finding replicates previous observations that we drew in frontotemporal dementia clinical variants,[5] strongly indicating the cerebellum as a key anatomical region to understand the pathophysiology of FTLD-related presentations.

Another fundamental goal of this work was to examine the association between healthy brain SFC architecture and the location of atrophy in PSP-RS, using the identified disease epicenter. In this study, we were able to demonstrate a strongly significant relationship between SFC architecture propagating from the left midbrain and atrophy distribution in patients with PSP-RS. This finding is consistent with recent evidence that a structural connectome-based network diffusion model propagating from a subcortical hypothalamic region could accurately predict the distribution of regional atrophy in patients with PSP,[7] supporting the hypothesis that pathological propagation of tau pathology in this disease may be caused by transsynaptic or transneuronal spreading neural connections at the basis of brain networks,[3,42] as previously demonstrated for Alzheimer's[49] disease and Parkinson's disease.[50] Our model was consistent with the pathological staging system proposed for PSP,[24] indicating early accumulation of 4R-tau burden primarily within subcortical regions (ie, midbrain, deep nuclei, cerebellum) and subsequent spreading to cortical regions only in later stages. This view is also consistent with longitudinal studies showing progression of brain atrophy within frontal and temporal regions, basal ganglia, midbrain, and cerebellum,[21] together with significant disruption over time of WM tracts, including the corpus callosum, superior longitudinal fasciculus, internal capsule, anterior thalamic radiation, and cerebellar peduncles.[51]

As a limitation of this study, its cross-sectional design prevented us from drawing firm conclusions about the development of functional connectivity alterations in PSP-RS, regarding their maladaptive or compensatory role in relationship with clinical progression. We also lack longitudinal validation of our model to predict the progression of atrophy over time. Indeed, the assumption that the peak of atrophy defines the disease epicenter is a mere simplification to suggest the possible region of maximal pathological burden. Another shortcoming lies in the fact that the AAL atlas does not include some subcortical regions that might be of interest in PSP-RS (eg, the subthalamic or brainstem nuclei), partially limiting our focus for correlations with atrophy. Nonetheless, we achieved the primary goals of our study, which were to propose SFC analysis as a new technique for assessing brain network disturbance in patients with PSP-RS and to support a network-based progression model in this disease. Our findings shed light on the architecture of functional disconnection in PSP-RS, which has the potential to be used to model disease development, track disease progression, and assess therapy response in future interventional studies.

Acknowledgments: We thank the patients and their families for the time and effort they dedicated to the research. Open access funding provided by BIBLIOSAN.

Author Contributions

M.F. and F.A. were responsible for study conception and design. E.G.S., A.G., I.B., S.B., E.C., and V.C. were responsible for acquisition and analyses of data. All authors were responsible for drafting or revising the text.

Data Availability Statement

The dataset used for this study will be made available by the corresponding author on request to qualified researchers (i.e., affiliated to a university or research institution/hospital).

References

1. Boxer AL, Yu JT, Golbe LI, Litvan I, Lang AE, Höglinger GU. Advances in progressive supranuclear palsy: new diagnostic criteria, biomarkers, and therapeutic approaches. Lancet Neurol 2017;16(7):552–563. https://doi.org/10.1016/s1474-4422(17)30157-6
2. Dickson DW, Kouri N, Murray ME, Josephs KA. Neuropathology of frontotemporal lobar degeneration-tau (FTLD-tau). J Mol Neurosci 2011;45(3):384–389. https://doi.org/10.1007/s12031-011-9589-0
3. Seeley WW, Crawford RK, Zhou J, Miller BL, Greicius MD. Neurodegenerative diseases target large-scale human brain networks. Neuron 2009;62(1):42–52. https://doi.org/10.1016/j.neuron.2009.03.024
4. Zuo XN, Ehmke R, Mennes M, et al. Network centrality in the human functional connectome. Cereb Cortex 2012;22(8):1862–1875. https://doi.org/10.1093/cercor/bhr269
5. Agosta F, Spinelli EG, Basaia S, et al. Functional Connectivity From Disease Epicenters in Frontotemporal Dementia. Neurology 2023;100(22):e2290–e2303. https://doi.org/10.1212/wnl.0000000000207277
6. Cope TE, Rittman T, Borchert RJ, et al. Tau burden and the functional connectome in Alzheimer's disease and progressive supranuclear palsy. Brain 2018;141(2):550–567. https://doi.org/10.1093/brain/awx347
7. Pandya S, Mezias C, Raj A. Predictive Model of Spread of Progressive Supranuclear Palsy Using Directional Network Diffusion. Original Research. Front Neurol 2017;8:692. https://doi.org/10.3389/fneur.2017.00692

8. Sepulcre J, Sabuncu MR, Yeo TB, Liu H, Johnson KA. Stepwise connectivity of the modal cortex reveals the multimodal organization of the human brain. J Neurosci 2012;32(31):10649–10661. https://doi.org/10.1523/JNEUROSCI.0759-12.2012
9. Costumero V, d'Oleire Uquillas F, Diez I, et al. Distance disintegration delineates the brain connectivity failure of Alzheimer's disease. Neurobiol Aging 2020;88:51–60. https://doi.org/10.1016/j.neurobiolaging.2019.12.005
10. Basaia S, Agosta F, Diez I, et al. Neurogenetic traits outline vulnerability to cortical disruption in Parkinson's disease. Neuroimage Clin 2022;33:102941. https://doi.org/10.1016/j.nicl.2022.102941
11. Höglinger GU, Respondek G, Stamelou M, et al. Clinical diagnosis of progressive supranuclear palsy: The movement disorder society criteria. Mov Disord 2017;32(6):853–864. https://doi.org/10.1002/mds.26987
12. Folstein MF, Folstein SE, McHugh PR. "Mini-mental state". A practical method for grading the cognitive state of patients for the clinician. J Psychiatr Res 1975;12(3):189–198.
13. The Unified Parkinson's Disease Rating Scale (UPDRS): status and recommendations. Mov Disord 2003;18(7):738–750. https://doi.org/10.1002/mds.10473
14. Goetz CG, Poewe W, Rascol O, et al. Movement Disorder Society Task Force report on the Hoehn and Yahr staging scale: status and recommendations. Mov Disord 2004;19(9):1020–1028. https://doi.org/10.1002/mds.20213
15. Ashburner J. A fast diffeomorphic image registration algorithm. Neuroimage 2007;38(1):95–113. https://doi.org/10.1016/j.neuroimage.2007.07.007
16. Santos-Santos MA, Mandelli ML, Binney RJ, et al. Features of Patients With Nonfluent/Agrammatic Primary Progressive Aphasia With Underlying Progressive Supranuclear Palsy Pathology or Corticobasal Degeneration. JAMA Neurol 2016;73(6):733–742. https://doi.org/10.1001/jamaneurol.2016.0412
17. Jenkinson M, Bannister P, Brady M, Smith S. Improved optimization for the robust and accurate linear registration and motion correction of brain images. Neuroimage 2002;17(2):825–841.
18. Andersson F, Joliot M, Perchey G, Petit L. Eye position-dependent activity in the primary visual area as revealed by fMRI. Hum Brain Mapp 2007;28(7):673–680. https://doi.org/10.1002/hbm.20296
19. Dutt S, Binney RJ, Heuer HW, et al. Progression of brain atrophy in PSP and CBS over 6 months and 1 year. Neurology 2016;87(19):2016–2025. https://doi.org/10.1212/wnl.0000000000003305
20. Höglinger GU, Schöpe J, Stamelou M, et al. Longitudinal magnetic resonance imaging in progressive supranuclear palsy: A new combined score for clinical trials. Mov Disord 2017;32(6):842–852. https://doi.org/10.1002/mds.26973
21. Nicastro N, Rodriguez PV, Malpetti M, et al. (18)F-AV1451 PET imaging and multimodal MRI changes in progressive supranuclear palsy. J Neurol 2020;267(2):341–349. https://doi.org/10.1007/s00415-019-09566-9
22. Zanigni S, Evangelisti S, Testa C, et al. White matter and cortical changes in atypical parkinsonisms: A multimodal quantitative MR study. Parkinsonism Relat Disord 2017;39:44–51. https://doi.org/10.1016/j.parkreldis.2017.03.001
23. Ishiki A, Harada R, Okamura N, et al. Tau imaging with [(18) F] THK-5351 in progressive supranuclear palsy. Eur J Neurol 2017;24(1):130–136. https://doi.org/10.1111/ene.13164
24. Kovacs GG, Lukic MJ, Irwin DJ, et al. Distribution patterns of tau pathology in progressive supranuclear palsy. Acta Neuropathol 2020;140(2):99–119. https://doi.org/10.1007/s00401-020-02158-2
25. Passamonti L, Vazquez Rodriguez P, Hong YT, et al. 18F-AV-1451 positron emission tomography in Alzheimer's disease and progressive supranuclear palsy. Brain 2017;140(3):781–791. https://doi.org/10.1093/brain/aww340
26. Williams DR, Holton JL, Strand C, et al. Pathological tau burden and distribution distinguishes progressive supranuclear palsy-parkinsonism from Richardson's syndrome. Brain 2007;130(6):1566–1576. https://doi.org/10.1093/brain/awm104
27. Bharti K, Bologna M, Upadhyay N, et al. Abnormal Resting-State Functional Connectivity in Progressive Supranuclear Palsy and Corticobasal Syndrome. Front Neurol 2017;8:248. https://doi.org/10.3389/fneur.2017.00248
28. Gardner RC, Boxer AL, Trujillo A, et al. Intrinsic connectivity network disruption in progressive supranuclear palsy. Ann Neurol 2013;73(5):603–616. https://doi.org/10.1002/ana.23844
29. Piattella MC, Tona F, Bologna M, et al. Disrupted resting-state functional connectivity in progressive supranuclear palsy. Am J Neuroradiol 2015;36(5):915–921. https://doi.org/10.3174/ajnr.A4229
30. Sintini I, Kaufman K, Botha H, et al. Neuroimaging correlates of gait abnormalities in progressive supranuclear palsy. Neuroimage Clin 2021;32:102850. https://doi.org/10.1016/j.nicl.2021.102850
31. Whitwell JL, Lowe VJ, Tosakulwong N, et al. [(18) F]AV-1451 tau positron emission tomography in progressive supranuclear palsy. Mov Disord 2017;32(1):124–133. https://doi.org/10.1002/mds.26834
32. Whitwell JL, Tosakulwong N, Botha H, et al. Brain volume and flortaucipir analysis of progressive supranuclear palsy clinical variants. Neuroimage Clin 2020;25:102152. https://doi.org/10.1016/j.nicl.2019.102152
33. Yoo HS, Chung SJ, Kim SJ, et al. The role of 18F-FP-CIT PET in differentiation of progressive supranuclear palsy and frontotemporal dementia in the early stage. Eur J Nucl Med Mol Imaging 2018;45(9):1585–1595. https://doi.org/10.1007/s00259-018-4019-y
34. Whitwell JL, Höglinger GU, Antonini A, et al. Radiological biomarkers for diagnosis in PSP: Where are we and where do we need to be? Mov Disord 2017;32(7):955–971. https://doi.org/10.1002/mds.27038
35. Agosta F, Sarasso E, Filippi M. Functional MRI in Atypical Parkinsonisms. Int Rev Neurobiol 2018;142:149–173. https://doi.org/10.1016/bs.irn.2018.09.002
36. Whitwell JL, Avula R, Master A, et al. Disrupted thalamocortical connectivity in PSP: a resting-state fMRI, DTI, and VBM study. Parkinsonism Relat Disord 2011;17(8):599–605. https://doi.org/10.1016/j.parkreldis.2011.05.013
37. Caso F, Agosta F, Volonté MA, et al. Cognitive impairment in progressive supranuclear palsy-Richardson's syndrome is related to white matter damage. Parkinsonism Relat Disord 2016;31:65–71. https://doi.org/10.1016/j.parkreldis.2016.07.007
38. Tessitore A, Giordano A, Caiazzo G, et al. Clinical correlations of microstructural changes in progressive supranuclear palsy. Neurobiol Aging 2014;35(10):2404–2410. https://doi.org/10.1016/j.neurobiolaging.2014.03.028
39. Agosta F, Sala S, Valsasina P, et al. Brain network connectivity assessed using graph theory in frontotemporal dementia. Neurology 2013;81(2):134–143. https://doi.org/10.1212/WNL.0b013e31829a33f8
40. Filippi M, Basaia S, Canu E, et al. Brain network connectivity differs in early-onset neurodegenerative dementia. Neurology 2017;89(17):1764–1772. https://doi.org/10.1212/WNL.0000000000004577
41. Douaud G, Filippini N, Knight S, Talbot K, Turner MR. Integration of structural and functional magnetic resonance imaging in amyotrophic lateral sclerosis. Brain 2011;134(Pt 12):3470–3479. https://doi.org/10.1093/brain/awr279
42. Fornito A, Zalesky A, Breakspear M. The connectomics of brain disorders. Nat Rev Neurosci 2015;16(3):159–172. https://doi.org/10.1038/nrn3901
43. Hakimi M, Maurer CW. Pseudobulbar Affect in Parkinsonian Disorders: A Review. J Mov Disord 2019;12(1):14–21. https://doi.org/10.14802/jmd.18051
44. Gorges M, Müller HP, Kassubek J. Structural and Functional Brain Mapping Correlates of Impaired Eye Movement Control in Parkinsonian Syndromes: A Systems-Based Concept. Front Neurol 2018;9:319. https://doi.org/10.3389/fneur.2018.00319
45. Rosskopf J, Gorges M, Müller HP, Pinkhardt EH, Ludolph AC, Kassubek J. Hyperconnective and hypoconnective cortical and subcortical functional networks in multiple system atrophy. Parkinsonism Relat Disord 2018;49:75–80. https://doi.org/10.1016/j.parkreldis.2018.01.012
46. Gellersen HM, Guo CC, O'Callaghan C, Tan RH, Sami S, Hornberger M. Cerebellar atrophy in neurodegeneration-a meta-analysis. J Neurol Neurosurg Psychiatry 2017;88(9):780–788. https://doi.org/10.1136/jnnp-2017-315607

47. Heleven E, van Dun K, Van Overwalle F. The posterior Cerebellum is involved in constructing Social Action Sequences: An fMRI Study. Sci Rep 2019;9(1):11110. https://doi.org/10.1038/s41598-019-46962-7

48. Metoki A, Wang Y, Olson IR. The Social Cerebellum: A Large-Scale Investigation of Functional and Structural Specificity and Connectivity. Cereb Cortex 2022;32(5):987–1003. https://doi.org/10.1093/cercor/bhab260

49. Filippi M, Basaia S, Canu E, et al. Changes in functional and structural brain connectome along the Alzheimer's disease continuum. Mol Psychiatry 2020;25(1):230–239. https://doi.org/10.1038/s41380-018-0067-8

50. Filippi M, Basaia S, Sarasso E, et al. Longitudinal brain connectivity changes and clinical evolution in Parkinson's disease. Mol Psychiatry 2021;26(9):5429–5440. https://doi.org/10.1038/s41380-020-0770-0

51. Agosta F, Caso F, Ječmenica-Lukić M, et al. Tracking brain damage in progressive supranuclear palsy: a longitudinal MRI study. J Neurol Neurosurg Psychiatry 2018;89(7):696–701. https://doi.org/10.1136/jnnp-2017-317443

Supporting Data

Additional Supporting Information may be found in the online version of this article at the publisher's web-site.